Discrimination of the effects of saturation and optical pumping in velocity-dependent pump-probe spectroscopy of rubidium: A simple analytical study

Heung-Ryoul Noh,[1,*] Geol Moon,[2] and Wonho Jhe[2,†]
[1]*Department of Physics, Chonnam National University, Gwangju 500-757, Korea*
[2]*School of Physics and Astronomy, Seoul National University, Seoul 151-747, Korea*
(Received 9 October 2010; published 27 December 2010)

This paper presents a simple analytical theory for the velocity-dependent pump-probe laser spectroscopy of ^{87}Rb and ^{85}Rb atoms where the pump and the probe beams are circularly or linearly polarized. The analytical solutions of the line shapes of the velocity-selective optical pumping spectroscopy [G. Moon and H. R. Noh, Phys. Rev. A **78**, 032506 (2008)] and saturated absorption spectroscopy [G. Moon and H. R. Noh, J. Opt. Soc. Am. B **25**, 701 (2008); **27**, 1741 (2010)] obtained in the previous reports, expressed as a sum of several Lorentzian functions, could be approximated as one (or in some cases, two) Lorentzian function(s). In particular, the contributions of the saturation and optical pumping effects could be discriminated explicitly in these simple analytical solutions, which is not possible in existing theories such as Nakayama's model. The simple analytical results for the saturation spectroscopy were compared with experimental results, and good agreement between them was observed.

DOI: 10.1103/PhysRevA.82.062517 PACS number(s): 32.30.−r, 32.70.Jz, 32.80.Xx, 42.62.Fi

I. INTRODUCTION

In velocity-dependent pump-probe laser spectroscopy, a weak probe beam detects the variation of the properties of the atomic vapor disturbed by a relatively intense pump beam [1]. Owing to the fact that only the atoms belonging to a specific velocity group can interact with the pump and probe beams simultaneously, a sub-Doppler resolution can be obtained in a normal Doppler broadened vapor cell. In usual velocity-selective optical pumping (VSOP) spectroscopy [2–11], the pump and probe beams have independent frequencies and propagate colinearly in either the same direction or opposite directions. If two beams originate from a single laser and propagate in opposite directions, we have the usual saturated absorption spectroscopy (SAS) [12–20]. Currently, VSOP and SAS are used widely in laser frequency stabilization [21] and spectroscopic measurement of the energy level of the atoms [3,22].

From a theoretical perspective, many methods to predict the line shape of the pump-probe spectroscopy spectrum have been developed. The usual method to calculate the line shape in the VSOP spectrum is the direct calculation of the density-matrix equation for the simplified model for real atoms [8–10]. However, many important properties such as the polarization dependence of the spectrum cannot be obtained using such a simplified model. In the case of the SAS spectrum, Nakayama developed a simple optical pumping model [23]. Based on Nakayama's model, Im *et al.* reported an analytical model for the SAS spectrum [16]. Although Nakayama's model predicts quite a reasonable SAS spectrum, it could not predict accurate line shapes, especially the linewidth of the spectrum. Moreover, Nakayama's model uses one Lorentzian function, while some real spectra for resonance or crossover lines cannot be expressed with a single Lorentzian function. There were also reports on direct calculation of the complicated density-matrix equations [18] and numerical calculation using rate equations [24].

Recently, Moon and Noh reported analytical solutions of the VSOP [25] and the SAS spectra [26,27]. After obtaining the analytical form of the population of each magnetic sublevel of the ground states in the presence of the pump beam, whose polarization is linear or circular, the transmission of a weak probe beam was calculated analytically. It was possible to predict the line shapes of the VSOP and the SAS spectra very accurately. Although it easily provides a prediction of the VSOP and the SAS spectra, the analytical form of the spectra consists of many Lorentzian functions, which can be an obstacle in using the analytical results in predicting the spectra. Extending the results obtained in the previous reports [25–27], in this paper, we present simple analytical solutions for the VSOP and the SAS spectra. The summation of many Lorentzian functions can be represented by one Lorentzian function, except for two cases in the SAS spectra of ^{87}Rb and ^{85}Rb atoms. In particular, the contribution of the optical pumping and saturation was discriminated explicitly, which was not available in existing theoretical models, such as Nakayama's model [23]. Once the signal is expressed in terms of one Lorentzian function, the width and the amplitude can be easily determined. This paper is structured as follows. Section II describes the theory for calculating simple analytical solutions of the VSOP and the SAS spectra. Typical examples for the VSOP and SAS spectra are presented in Sec. III. Section IV presents a comparison between the analytical and experimental results for the SAS spectra. The final section summarizes the results.

II. THEORY

The energy-level diagram of ^{87}Rb and ^{85}Rb atoms under consideration is shown in Fig. 1. We consider a pump and a probe beam either in a counterpropagating or copropagating geometry. To obtain an analytical solution of the spectrum, the polarization of the pump beam was assumed to be circular

*hrnoh@chonnam.ac.kr
†whjhe@snu.ac.kr

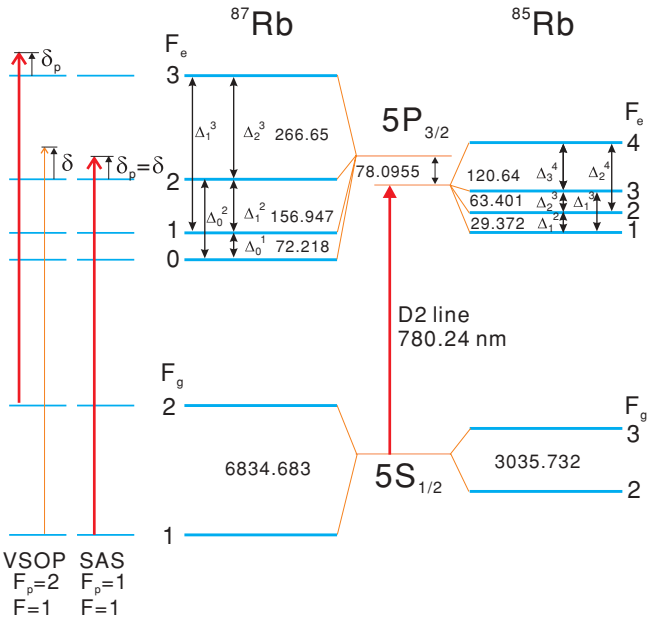

FIG. 1. (Color online) The energy-level diagrams used in calculating VSOP and SAS spectra. The numbers denote the frequency spacing in units of megahertz.

or linear. In VSOP spectroscopy, the pump and the probe beams are tuned to the transitions from the ground state of the angular momentum quantum number $F_g = F_p$ and $F_g = F$, respectively. F_p and F can be $I \pm (1/2)$, where I is the nuclear angular momentum quantum number of the atom. Since the pump and probe beams are derived from a laser in the SAS, we have $F_p = F$. Therefore, it was possible to construct a single formalism which could be used in both VSOP and SAS.

From the previous reports, the analytical form of the absorption coefficient of a weak probe beam, averaged over a Maxwell-Boltzmann velocity distribution, for the transition $F_g \to F_e = F_g - 1, F_g, F_g + 1$ of the D_2 transition of alkali-metal atoms, in the presence of a pump beam, can be described as follows (Eq. (14) of Ref. [25]):

$$\alpha = \alpha_{\rm BG} + C_0 \sum_{\nu=F-1}^{F+1} D_\nu^{F+1} \sum_{\mu=F_p-1}^{F_p+1} \sum_{m=-F}^{F} R_{F,m}^{\nu,m+q} \times M_{F_p\to\mu}^{(F,m)}\left[\delta + \Delta_\nu^{F+1} \pm \left(\delta_p + \Delta_\mu^{F_p+1}\right)\right], \quad (1)$$

where the probe (pump) beam is tuned to the transition from the ground state of $F_g = F$ (F_p). The upper (lower) sign represents the counterpropagating (copropagating) scheme in Eq. (1). In Eq. (1), $C_0 = \frac{3\lambda^2}{2\pi}\frac{N_{\rm at}}{\sqrt{\pi}u}\frac{\pi\Gamma}{2k}$, λ is the resonant wavelength, $N_{\rm at}$ is the atomic density, Γ is the decay rate of the excited state, k ($=2\pi/\lambda$) is the wave vector, and $u = (2k_BT/M)^{1/2}$ is the most probable velocity (T, temperature of the cell; M, mass of an atom). The Doppler factor is given by

$$D_n^m = \exp\left[-\left(\frac{\delta + \Delta_n^m}{ku}\right)^2\right].$$

$R_{F_g,m_g}^{F_e,m_e}$ is the normalized transition strength between the states $|F_g,m_g\rangle$ and $|F_e,m_e\rangle$ and is given by [28]

$$R_{F_g,m_g}^{F_e,m_e} = (2L_e+1)(2J_e+1)(2J_g+1)(2F_e+1)(2F_g+1) \times \left[\begin{Bmatrix} L_e & J_e & S \\ J_g & L_g & 1 \end{Bmatrix}\begin{Bmatrix} J_e & F_e & I \\ F_g & J_g & 1 \end{Bmatrix} \times \begin{pmatrix} F_g & 1 & F_e \\ m_g & m_e - m_g & -m_e \end{pmatrix}\right]^2,$$

where L and S represent the orbital and electron spin angular momenta, respectively, and $\{\cdots\}$ and $(\cdots)$ denote the $6J$ and $3J$ symbols, respectively. In Eq. (1), $M_{F_p\to\mu}^{(F,m)}$ is the contribution of the magnetic sublevel of the ground state, $|F,m\rangle$, to the absorption coefficient, and is derived from the convolution integral of the absorption cross section and the population of the ground state. $M_{F_p\to\mu}^{(F,m)}$ is composed of several Lorentzian functions, whose explicit form can be found in the appendix of Ref. [25]. δ (δ_p) is the detuning of the probe (pump) beam relative to the transition between $F_g \to F_e = F_g + 1$, and $\hbar\Delta_{F_e}^{F_e'} = E_{F_e'} - E_{F_e}$ is the hyperfine energy spacing of the excited states. In the case of the SAS spectrum, $\delta = \delta_p$, $F = F_p$, and the + sign is used in Eq. (1).

In Eq. (1), $\alpha_{\rm BG}$ denotes the background absorption coefficient in the absence of the pump beam and is explicitly given by

$$\alpha_{\rm BG} = \begin{cases} \frac{1}{8}C_0\left(\frac{5}{6}D_2^2 + \frac{5}{6}D_1^2 + \frac{1}{3}D_0^2\right), & \text{for } F = 1, \\ \frac{1}{8}C_0\left(\frac{7}{3}D_3^3 + \frac{5}{6}D_2^3 + \frac{1}{6}D_1^3\right), & \text{for } F = 2, \end{cases}$$

for ^{87}Rb atoms. In the case of ^{85}Rb atoms, it is given by

$$\alpha_{\rm BG} = \begin{cases} \frac{1}{12}C_0\left(\frac{28}{27}D_3^3 + \frac{35}{27}D_2^3 + D_1^3\right), & \text{for } F = 2, \\ \frac{1}{12}C_0\left(3D_4^4 + \frac{35}{27}D_3^4 + \frac{10}{27}D_2^4\right), & \text{for } F = 3. \end{cases}$$

It should be noted that C_0 for ^{87}Rb atoms differs from that for ^{85}Rb atoms.

We now discuss how to express the sum of Lorentzian functions shown in Eq. (1) as a single Lorentzian function. The line-shape function of VSOP or SAS is composed of various Lorentzian functions, corresponding to the imaginary part of the function

$$L(a,b) \simeq \frac{b}{\sqrt{1+b}}\frac{1}{2a + i(1+\sqrt{1+b})}, \quad (2)$$

where a is the normalized frequency and $1 + (b+1)^{1/2}$ is the normalized linewidth. In the case of the Lorentzian function associated with saturation effect, b is the on-resonance saturation parameter, $s_0 = I_p/I_s$ (I_p, intensity of the pump beam; I_s, the saturation intensity). In contrast, the function related to the optical pumping consists of the product of the interaction time and saturation parameter and is usually much larger than unity. Let us consider the sum of the functions like Eq. (2) with different linewidths, as given by

$$Q = \sum_n c_n L(a,b_n),$$

where c_n and $1 + (b_n+1)^{1/2}$ represent the amplitude and the normalized width of the nth function. Provided that the

magnitudes of the linewidths are not too different from each other, the reciprocal of Q can be expanded in powers of a up to first order in a, as follows:

$$Q^{-1} = Q^{-1}(a=0) + \left.\frac{dQ^{-1}}{da}\right|_{a=0} a + O(a^2).$$

Therefore,

$$\begin{aligned} Q &\simeq \left(Q^{-1}(a=0) + \left.\frac{dQ^{-1}}{da}\right|_{a=0} a \right)^{-1} \\ &= cL\,(a,b)\,, \end{aligned} \tag{3}$$

where the amplitude (c) and the width (b) are given by

$$c \simeq \sum_n c_n, \quad b \simeq c^2 \left(\sum_n \frac{c_n}{\sqrt{b_n}} \right)^{-2}, \tag{4}$$

respectively. If the imaginary part of Eq. (3) is taken, finally the following equation can be obtained:

$$\sum_n c_n L_i(a,b_n) \simeq cL_i(a,b), \tag{5}$$

where the effective amplitude, c, and linewidth, b, are given in Eq. (4). $L_i(a,b)$ is the imaginary part of the function $L(a,b)$ in Eq. (2) and is given by the following:

$$L_i\,(a,b) \simeq -\frac{b}{\sqrt{1+b}} \frac{1+\sqrt{1+b}}{4a^2 + (1+\sqrt{1+b})^2}. \tag{6}$$

III. CALCULATED RESULTS

We now apply the technique developed in the preceding section for the analytical solutions of VSOP and SAS spectra. The explicit analytical form of the absorption coefficient for $F_p = 2$ and $F = 1$ of ^{87}Rb atoms in a copropagating scheme where both the pump and probe beams are σ^+ polarized is given by the following [25]:

$$\begin{aligned} \alpha_{\mathrm{VSOP}}(\delta) = \alpha_{\mathrm{BG}} + C_0 \big[& D_2^2 S_1\big(\delta - \delta_p - \Delta_1^3\big) \\ & + D_2^2 S_{2a}\big(\delta - \delta_p - \Delta_2^3\big) + D_1^2 S_{2b}\big(\delta - \delta_p - \Delta_2^3\big) \\ & + D_0^2 S_3\big(\delta - \delta_p - \Delta_2^3 + \Delta_0^1\big) \\ & + D_1^2 S_4\big(\delta - \delta_p - \Delta_2^3 + \Delta_1^2\big) \\ & + D_0^2 S_5\big(\delta - \delta_p - \Delta_2^3 + \Delta_0^2\big)\big]. \end{aligned} \tag{7}$$

In Eq. (7),

$$\begin{aligned} S_1(\Delta) = & -\frac{2145}{47\,488} L_i\left(\frac{\Delta}{\Gamma}, \frac{59}{7200}\tau\right) \\ & - \frac{275}{8064} L_i\left(\frac{\Delta}{\Gamma}, \frac{19}{800}\tau\right) - \frac{295}{17\,172} L_i\left(\frac{\Delta}{\Gamma}, \frac{9}{200}\tau\right), \end{aligned}$$

$$S_{2a}(\Delta) = -\frac{103}{784} L_i\left(\frac{\Delta}{\Gamma}, \frac{5}{72}\tau\right) + \frac{149}{21\,168} L_i\left(\frac{\Delta}{\Gamma}, \frac{3}{32}\tau\right),$$

$$\begin{aligned} S_{2b}(\Delta) = & -\frac{3575}{142\,464} L_i\left(\frac{\Delta}{\Gamma}, \frac{59}{7200}\tau\right) - \frac{375}{15\,232} L_i\left(\frac{\Delta}{\Gamma}, \frac{19}{800}\tau\right) \\ & - \frac{54\,575}{1\,167\,696} L_i\left(\frac{\Delta}{\Gamma}, \frac{9}{200}\tau\right), \end{aligned} \tag{8}$$

$$\begin{aligned} S_3(\Delta) = & -\frac{25}{1224} L_i\left(\frac{\Delta}{\Gamma}, \frac{19}{800}\tau\right) - \frac{25}{1377} L_i\left(\frac{\Delta}{\Gamma}, \frac{9}{200}\tau\right), \\ S_4(\Delta) = & -\frac{1}{16} L_i\left(\frac{\Delta}{\Gamma}, \frac{5}{72}\tau\right) - \frac{5}{216} L_i\left(\frac{\Delta}{\Gamma}, \frac{3}{32}\tau\right), \\ S_5(\Delta) = & -\frac{1}{70} L_i\left(\frac{\Delta}{\Gamma}, \frac{5}{72}\tau\right) - \frac{5}{1512} L_i\left(\frac{\Delta}{\Gamma}, \frac{3}{32}\tau\right), \end{aligned}$$

where $\tau = s_0 \Gamma t$, Γ is the decay rate of the excited state and $t = (\sqrt{\pi}/2)d/u$ is the average transit time crossing the pump beam (d, the pump beam diameter) [29].

As an example, let us consider the signal $S_1(\Delta)$ in Eq. (8). Using Eq. (4), we have

$$\begin{aligned} c &= -\frac{125}{1296}, \\ b &= \frac{77\,834\,395\,746\,450}{9(7\,407\,568 + 4\,643\,595\sqrt{19} + 5\,942\,079\sqrt{59})^2} \\ &\simeq 0.0145. \end{aligned}$$

Because the exact form of the values is of no importance, b can be expressed by $b \simeq 145/10\,000$. In what follows, we express the complicated numbers within three significant digits. Therefore, we have

$$S_1(\Delta) = -\frac{125}{1296} L_i\left(\frac{\Delta}{\Gamma}, \frac{145}{10\,000}\tau\right).$$

All the signals are then given by

$$\begin{aligned} S_1(\Delta) &= -\frac{125}{1296} L_i\left(\frac{\Delta}{\Gamma}, \frac{145}{10\,000}\tau\right), \\ S_{2a}(\Delta) &= -\frac{47}{378} L_i\left(\frac{\Delta}{\Gamma}, \frac{683}{10\,000}\tau\right), \\ S_{2b}(\Delta) &= -\frac{125}{1296} L_i\left(\frac{\Delta}{\Gamma}, \frac{215}{10\,000}\tau\right), \\ S_3(\Delta) &= -\frac{25}{648} L_i\left(\frac{\Delta}{\Gamma}, \frac{313}{10\,000}\tau\right), \\ S_4(\Delta) &= -\frac{37}{432} L_i\left(\frac{\Delta}{\Gamma}, \frac{750}{10\,000}\tau\right), \\ S_5(\Delta) &= -\frac{19}{1080} L_i\left(\frac{\Delta}{\Gamma}, \frac{732}{10\,000}\tau\right). \end{aligned} \tag{9}$$

The comparison between Eqs. (8) and (9) are given later in this section.

The general analytical form of the SAS spectrum for the transition $F_g = F \to F_e = F-1$, F, and $F+1$ for the D_2 of the alkali-metal atoms is given by the following [26]:

$$\begin{aligned} \alpha_{\mathrm{SAS}}(\delta) = \alpha_{\mathrm{BG}} + C_0 \big[& S_{F+1}(2\delta) + S_F\big(2\delta + 2\Delta_F^{F+1}\big) \\ & + S_{F-1}\big(2\delta + 2\Delta_{F-1}^{F+1}\big) \\ & + D_F^{F+1} C_F^{F+1}\big(2\delta + \Delta_F^{F+1}\big) \\ & + D_{F-1}^{F+1} C_{F-1}^{F+1}\big(2\delta + \Delta_{F-1}^{F+1}\big) \\ & + D_{F-1}^{F} C_{F-1}^{F}\big(2\delta + \Delta_{F-1}^{F+1} + \Delta_F^{F+1}\big)\big], \end{aligned} \tag{10}$$

where δ is the detuning of the laser beam relative to the transition between $F_g = F \to F_e = F+1$, and $D_F^{F'} = \exp\left[-(\Delta_F^{F'}/2ku)^2\right]$ is the Doppler factor. Note that a

different form of the Doppler factor was used to that defined in Sec. II.

As a second example, we apply the technique for the analytical solutions of the SAS spectrum for the transition $F_g = 1 \rightarrow F_e = 0,1,2$ of ^{87}Rb atoms when both the pump and probe beams are σ^+ polarized. In Eq. (10), the analytical solutions of the three resonance (S_2, S_1, and S_0) signals and three crossover (C_1^2, C_0^2, and C_0^1) signals are given by the following:

$$
\begin{aligned}
S_2(\Delta) &= \frac{253}{9600} L_i\left(\frac{\Delta}{\Gamma}, \frac{11}{288}\tau\right) + \frac{9}{128} L_i\left(\frac{\Delta}{\Gamma}, \frac{3}{32}\tau\right) \\
&\quad + \frac{3}{400} L_i\left(\frac{\Delta}{\Gamma}, \frac{1}{8}\tau\right), \\
S_1(\Delta) &= \frac{5}{48} L_i\left(\frac{\Delta}{\Gamma}, \frac{35}{288}\tau\right), \\
S_0(\Delta) &= \frac{1}{24} L_i\left(\frac{\Delta}{\Gamma}, \frac{1}{9}\tau\right), \\
C_1^2(\Delta) &= -\frac{1}{21} L_i\left(\frac{\Delta}{\Gamma}, \frac{35}{288}\tau\right) + \frac{25}{384} L_i\left(\frac{\Delta}{\Gamma}, \frac{11}{288}\tau\right) \\
&\quad + \frac{5}{128} L_i\left(\frac{\Delta}{\Gamma}, \frac{3}{32}\tau\right), \\
C_0^2(\Delta) &= -\frac{7}{192} L_i\left(\frac{\Delta}{\Gamma}, \frac{1}{9}\tau\right) + \frac{1}{24} L_i\left(\frac{\Delta}{\Gamma}, \frac{11}{288}\tau\right), \\
C_0^1(\Delta) &= \frac{5}{192} L_i\left(\frac{\Delta}{\Gamma}, \frac{1}{9}\tau\right) + \frac{1}{24} L_i\left(\frac{\Delta}{\Gamma}, \frac{35}{288}\tau\right).
\end{aligned} \tag{11}
$$

By using the same method used in the calculation of VSOP spectra, Eq. (11) can be expressed as follows:

$$
\begin{aligned}
S_2(\Delta) &= \frac{5}{48} L_i\left(\frac{\Delta}{\Gamma}, \frac{729}{10\,000}\tau\right), \\
S_1(\Delta) &= \frac{5}{48} L_i\left(\frac{\Delta}{\Gamma}, \frac{35}{288}\tau\right), \\
S_0(\Delta) &= \frac{1}{24} L_i\left(\frac{\Delta}{\Gamma}, \frac{1}{9}\tau\right), \\
C_1^2(\Delta) &= \frac{19}{336} L_i\left(\frac{\Delta}{\Gamma}, \frac{304}{10\,000}\tau\right), \\
C_0^2(\Delta) &= \frac{1}{24} L_i\left(\frac{\Delta}{\Gamma}, \frac{11}{288}\tau\right) - \frac{7}{192} L_i\left(\frac{\Delta}{\Gamma}, \frac{1}{9}\tau\right), \\
C_0^1(\Delta) &= \frac{13}{192} L_i\left(\frac{\Delta}{\Gamma}, \frac{117}{1000}\tau\right),
\end{aligned} \tag{12}
$$

It was not possible to express the crossover signal C_0^2 by a single function. This was because the constants representing linewidth were significantly different from each other and had opposite signs. There does not exist a clear criterion for distinguishing the two cases. However, we found that most signals relying on optical pumping can be described by one Lorentzian function, except for the two cases in the SAS spectra of ^{87}Rb and ^{85}Rb atoms.

The validity of the calculation is shown in Fig. 2. Figures 2(a) and 2(b) show the analytical results of the VSOP and SAS spectra, respectively. In Fig. 2, the Doppler backgrounds were subtracted for brevity, and all the beams were assumed to be σ^+ polarized. Figure 2(a) shows the absorption coefficient for VSOP spectroscopy in the copropagating scheme where the

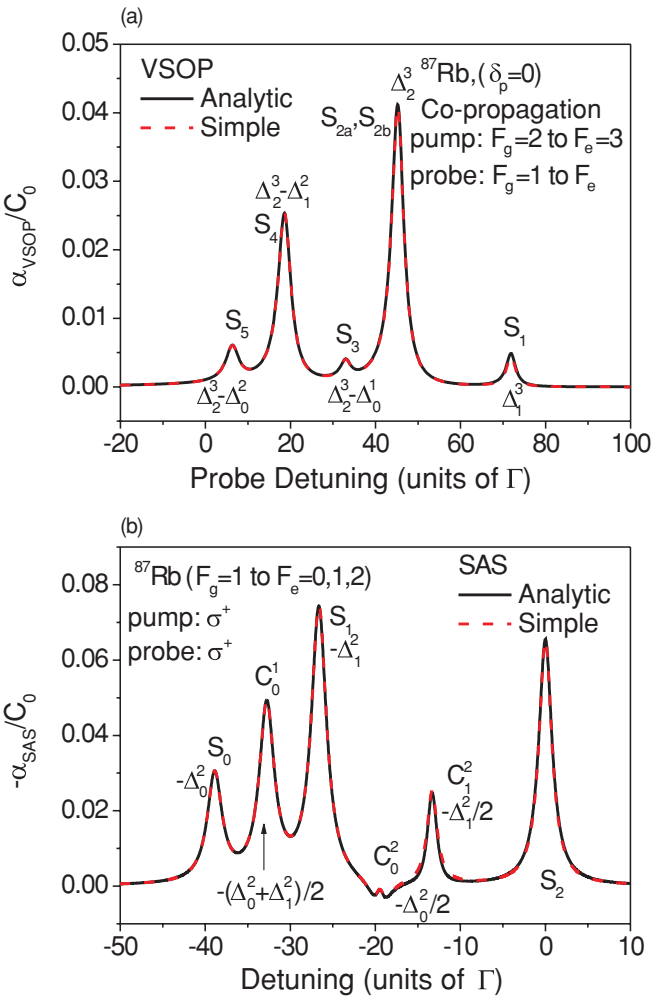

FIG. 2. (Color online) (a) [(b)] Comparison between the analytical results in Eq. (8) [Eq. (11)] and simple analytical results in Eq. (9) [Eq. (12)] for the VSOP [SAS] spectra.

pump beam is fixed at the resonant transition line $F_g = 2 \rightarrow F_e = 3$ and the probe beam is scanned around the transition $F_g = 1 \rightarrow F_e$. Figure 2(b) shows the inverted absorption coefficient for the SAS at the transition $F_g = 1 \rightarrow F_e$. In Fig. 2(a) and 2(b), the solid and dashed curves denote the results in Eq. (8) [Eq. (11)] and Eq. (9) [Eq. (12)], respectively. We can clearly see the validity of the approximation used in the calculation. The comparison for other SAS spectra is presented in the next section along with experimental results.

All terms in Eq. (12) depend on τ, which implies that the signals originate from the optical pumping rather than the saturation effect. Some signals for other polarization configurations have the effects of both optical pumping and saturation. For example, let us consider the signal for the transition $F_g = 2 \rightarrow F_e = 3$ of ^{87}Rb atoms when the pump and probe beams are σ^+ polarized. As shown in Eq. (29) of Ref. [26], the line shape can be describe by the following:

$$
\begin{aligned}
&\frac{5}{8} L_i\left(\frac{\Delta}{\Gamma}, s_0\right) + \frac{5}{16} L_i\left(\frac{\Delta}{\Gamma}, \frac{\tau}{9}\right) - \frac{127}{440} L_i\left(\frac{\Delta}{\Gamma}, \frac{2}{25}\tau\right) \\
&\quad - \frac{119}{800} L_i\left(\frac{\Delta}{\Gamma}, \frac{3}{25}\tau\right) - \frac{5503}{26\,400} L_i\left(\frac{\Delta}{\Gamma}, \frac{7}{225}\tau\right),
\end{aligned} \tag{13}
$$

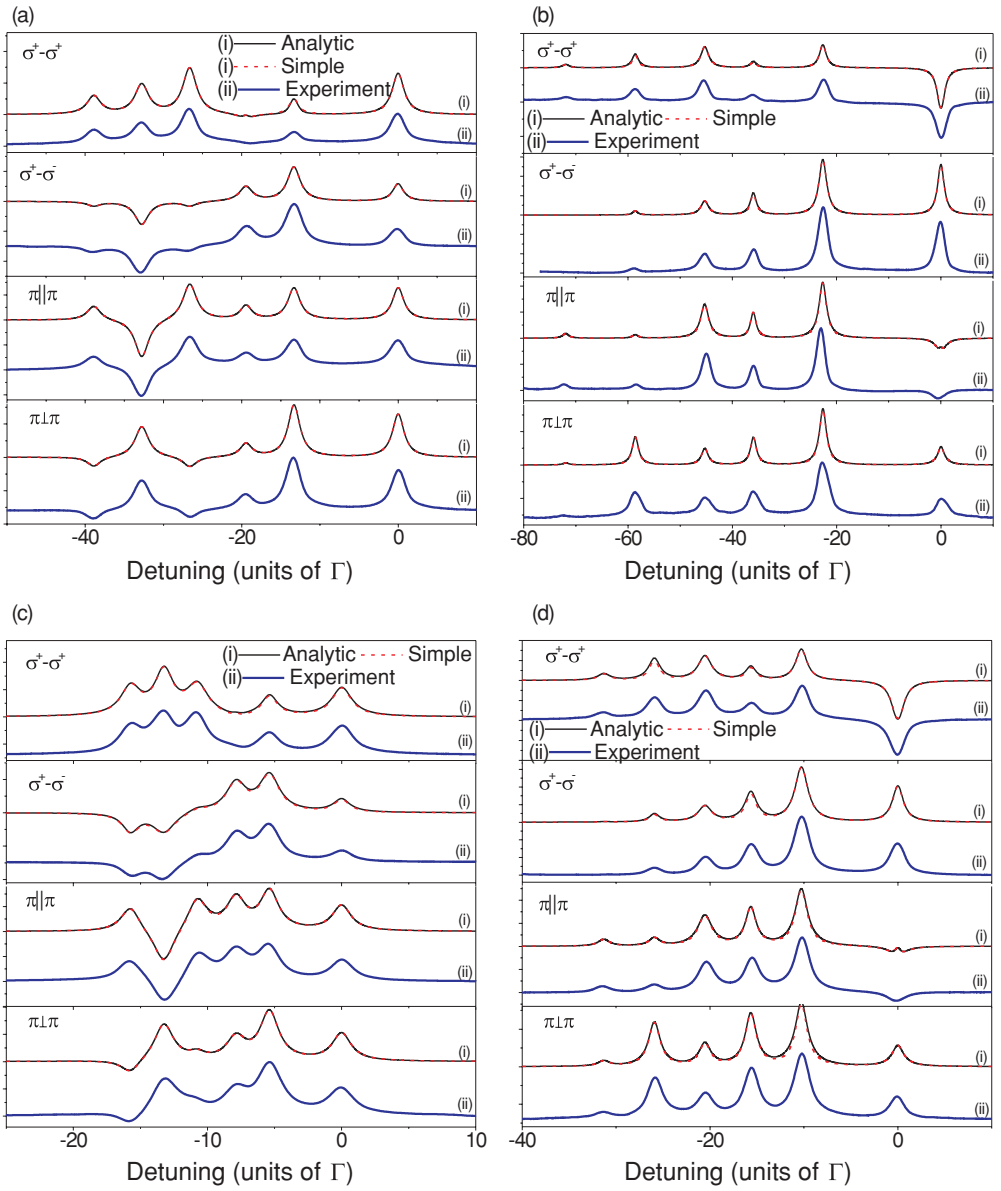

FIG. 3. (Color online) Comparison of analytical results of the SAS with experimental results for the transition (a) $F_g = 1 \rightarrow F_e = 0,1,2$ of ^{87}Rb atoms, (b) $F_g = 2 \rightarrow F_e = 1,2,3$ of ^{87}Rb atoms, (c) $F_g = 2 \rightarrow F_e = 1,2,3$ of ^{85}Rb atoms, and (d) $F_g = 3 \rightarrow F_e = 2,3,4$ of ^{85}Rb atoms.

where the term regarding the effect of the light pressure has been ignored. In Eq. (13), the first term denotes the saturation effect, whereas the other terms represent the effect of optical pumping. Following the method described in Sec. II, Eq. (13) can be expressed as follows:

$$\frac{5}{8}L_i\left(\frac{\Delta}{\Gamma},s_0\right)-\frac{1}{3}L_i\left(\frac{\Delta}{\Gamma},\frac{387}{10\,000}\tau\right). \qquad (14)$$

In Eq. (14), the first and second terms denote the effects of the saturation and optical pumping, respectively. Therefore, we could discriminate between the effects of saturation and optical pumping explicitly for specific signals whenever both effects exist together. As shown in the appendix, many signals are composed of terms due to these two effects.

The results for the other transitions of ^{87}Rb and ^{85}Rb atoms in the σ^+–$\sigma^\pm$, $\pi \parallel \pi$, and $\pi \perp \pi$ configurations are listed in the appendix. The numerical values in the appendix were derived from the results in Refs. [26,30] using the method described in this section. It was concluded that all the resonance and crossover signals consist of one or two Lorentzian functions.

IV. COMPARISON WITH EXPERIMENTAL RESULTS

In this section, we compare the analytical results for the SAS spectra presented in Ref. [26], the simple analytical results obtained in this paper, and experimental results. The experimental setup and procedure is similar to those in [26,31]. Here, we describe the experimental methods only briefly. All the laser beams (pump, probe, and reference) were derived from an external cavity diode laser (TOPTICA, DL100). The difference in the transmission of the probe and

reference beam counterpropagating to the pump beam was measured with a photodiode. The rubidium cell was placed at room temperature. In order to eliminate the terrestrial magnetic field, we wrapped the cell with a μ-metal sheet. The intensity of the pump (probe) beam was 3.2 μW/mm^2 (3.0×10^{-2} μW/mm^2). The diameters of the pump and probe beams were 3.0 mm.

The results of ^{87}Rb [^{85}Rb] atoms for the transitions from the lower and upper ground states are presented in Figs. 3(a) and 3(b) [Figs. 3(c) and 3(d)], respectively. In each panel in Fig. 3, the results for the pump-probe polarization configurations of $\sigma^+-\sigma^+$, $\sigma^+-\sigma^-$, $\pi\parallel\pi$, and $\pi\perp\pi$ are presented in descending order from top to bottom. In Fig. 3, the analytical, simple analytical, and experimental results are shown as black solid, red dotted, and blue solid curves, respectively. In each panel, the upper figure [(i)] shows the analytical results superimposed with the simple analytical results and the lower one [(ii)] presents the experimental results. It easily is seen that the analytical and simple analytical results agree with each other. We also find that the analytical results are in good agreement with experimental results. It should be noted that the slightly larger linewidths in the experimental results than in the analytical results could be attributed to laser linewidths ($\sim$1 MHz) and saturation effect, which were not completely accounted for in our theory.

V. CONCLUSIONS

In this paper, we have presented a simple analytical theory of velocity-selective optical pumping spectroscopy and saturation spectroscopy. After solving the rate equations for the population of the atoms and establishing the analytical forms of the VSOP and SAS spectra, the obtained results, composed of many Lorentzian functions with different amplitudes and linewidths, could be expressed as one (or two, for special cases) Lorentzian function(s). In particular, the effects of saturation and optical pumping could be explicitly discriminated. This could not be accomplished by Nakayama's model. Although the calculation has been carried out for ^{87}Rb and ^{85}Rb atoms, these results for the SAS spectra are valid for alkali-metal atoms with $I=3/2$ and $I=5/2$, respectively. Therefore, the results for ^{87}Rb are directly applicable to atoms such as ^{7}Li, ^{27}Na, and ^{39}K by employing different values of frequencies. As well as providing a simple and succinct understanding of the saturation and optical pumping spectroscopy, this method could be used to easily predict the spectrum and extended to other spectroscopic techniques such as polarization spectroscopy.

ACKNOWLEDGMENT

This work was supported by the Korea Research Foundation Grant funded by the Korean government (KRF-2008-313-C00355).

APPENDIX

The simple analytical results for the SAS spectra in Eq. (10) for ^{87}Rb and ^{85}Rb atoms are presented in this appendix. For brevity, Δ/Γ in $L_i(\Delta/\Gamma,b)$ is omitted.

(i) The transition $F_g=1\rightarrow F_e=0,1,2$ of ^{87}Rb atoms for the σ^+–σ^- pump-probe polarization configuration:

$$S_2=\frac{5}{48}L_i\left(\frac{486}{10\,000}\tau\right),\quad S_1=-\frac{5}{224}L_i\left(\frac{35}{288}\tau\right),$$
$$S_0=-\frac{1}{48}L_i\left(\frac{1}{9}\tau\right),\quad C_1^2=\frac{41}{224}L_i\left(\frac{930}{10\,000}\tau\right),\quad\text{(A1)}$$
$$C_0^2=\frac{1}{12}L_i\left(\frac{960}{10\,000}\tau\right),\quad C_0^1=-\frac{25}{224}L_i\left(\frac{116}{1000}\tau\right).$$

(ii) The transition $F_g=1\rightarrow F_e=0,1,2$ of ^{87}Rb atoms for the $\pi||\pi$ polarization configuration:

$$S_2=\frac{5}{48}L_i\left(\frac{691}{10\,000}\tau\right),\quad S_1=\frac{5}{48}L_i\left(\frac{35}{288}\tau\right),$$
$$S_0=\frac{1}{24}L_i\left(\frac{1}{9}\tau\right),\quad C_1^2=\frac{3}{28}L_i\left(\frac{779}{10\,000}\tau\right),\quad\text{(A2)}$$
$$C_0^2=\frac{5}{96}L_i\left(\frac{662}{10\,000}\tau\right),\quad C_0^1=-\frac{25}{224}L_i\left(\frac{116}{1000}\tau\right).$$

(iii) The transition $F_g=1\rightarrow F_e=0,1,2$ of ^{87}Rb atoms for the $\pi\perp\pi$ polarization configuration:

$$S_2=\frac{5}{48}L_i\left(\frac{710}{10\,000}\tau\right),\quad S_1=-\frac{5}{224}L_i\left(\frac{35}{288}\tau\right),$$
$$S_0=-\frac{1}{48}L_i\left(\frac{1}{9}\tau\right),\quad C_1^2=\frac{89}{672}L_i\left(\frac{753}{10\,000}\tau\right),\quad\text{(A3)}$$
$$C_0^2=\frac{7}{192}L_i\left(\frac{735}{10\,000}\tau\right),\quad C_0^1=\frac{13}{192}L_i\left(\frac{117}{1000}\tau\right).$$

(iv) The transition $F_g=2\rightarrow F_e=1,2,3$ of ^{87}Rb atoms for the σ^+–σ^+ polarization configuration:

$$S_3=\frac{5}{8}L_i(s_0)-\frac{1}{3}L_i\left(\frac{387}{10\,000}\tau\right),\quad S_2=\frac{83}{840}L_i\left(\frac{707}{10\,000}\tau\right),$$
$$S_1=\frac{1}{48}L_i\left(\frac{277}{10\,000}\tau\right),\quad C_2^3=\frac{253}{1680}L_i\left(\frac{445}{10\,000}\tau\right),$$
$$C_1^3=\frac{35}{432}L_i\left(\frac{150}{10\,000}\tau\right),\quad C_1^2=\frac{11}{108}L_i\left(\frac{195}{10\,000}\tau\right).\quad\text{(A4)}$$

(v) The transition $F_g=2\rightarrow F_e=1,2,3$ of ^{87}Rb atoms for the σ^+–σ^- polarization configuration:

$$S_3=\frac{1}{48}L_i(s_0)+\frac{1}{4}L_i\left(\frac{382}{10\,000}\tau\right),$$
$$S_2=\frac{593}{10\,080}L_i\left(\frac{675}{10\,000}\tau\right),\quad S_1=0,$$
$$C_2^3=\frac{5}{96}L_i(s_0)+\frac{1703}{6300}L\left(\frac{736}{10\,000}\tau\right),\quad\text{(A5)}$$
$$C_1^3=\frac{1}{32}L_i(s_0)+\frac{23}{108}L_i\left(\frac{205}{10\,000}\tau\right),$$
$$C_1^2=\frac{6523}{151\,200}L_i\left(\frac{972}{100\,000}\tau\right).$$

(vi) The transition $F_g = 2 \rightarrow F_e = 1,2,3$ of ^{87}Rb atoms for the $\pi||\pi$ polarization configuration:

$$S_3 = \frac{315}{922}L_i\left(\frac{252}{461}s_0\right) - \frac{553}{11\,064}L_i\left(\frac{110}{1000}\tau\right),$$
$$S_2 = \frac{5}{48}L_i\left(\frac{689}{10\,000}\tau\right), \quad S_1 = \frac{1}{48}L_i\left(\frac{251}{10\,000}\tau\right),$$
$$C_2^3 = \frac{615}{14\,752}L_i\left(\frac{252}{461}s_0\right) + \frac{219}{1000}L_i\left(\frac{548}{10\,000}\tau\right),$$
$$C_1^3 = \frac{1475}{44\,256}L_i\left(\frac{252}{461}s_0\right) + \frac{187}{1000}L_i\left(\frac{232}{10\,000}\tau\right),$$
$$C_1^2 = \frac{174}{10\,000}L_i\left(\frac{222}{10\,000}\tau\right). \tag{A6}$$

(vii) The transition $F_g = 2 \rightarrow F_e = 1,2,3$ of ^{87}Rb atoms for the $\pi\perp\pi$ polarization configuration:

$$S_3 = \frac{753}{3688}L_i\left(\frac{252}{461}s_0\right) + \frac{553}{22\,128}L_i\left(\frac{110}{1000}\tau\right),$$
$$S_2 = \frac{2909}{60\,672}L_i\left(\frac{381}{10\,000}\tau\right), \quad S_1 = \frac{1}{144}L_i\left(\frac{243}{10\,000}\tau\right),$$
$$C_2^3 = \frac{3995}{29\,504}L_i\left(\frac{252}{461}s_0\right) + \frac{170}{1000}L_i\left(\frac{483}{10\,000}\tau\right),$$
$$C_1^3 = \frac{5521}{232\,344}L_i\left(\frac{252}{461}s_0\right) + \frac{150}{1000}L_i\left(\frac{258}{10\,000}\tau\right),$$
$$C_1^2 = \frac{981}{10\,000}L_i\left(\frac{284}{10\,000}\tau\right). \tag{A7}$$

(viii) The transition $F_g = 2 \rightarrow F_e = 1,2,3$ of ^{85}Rb atoms for the σ^+–σ^+ polarization configuration:

$$S_3 = \frac{7}{81}L_i\left(\frac{642}{10\,000}\tau\right), \quad S_2 = \frac{10\,213}{123\,120}L_i\left(\frac{914}{10\,000}\tau\right),$$
$$S_1 = \frac{1}{12}L_i\left(\frac{684}{10\,000}\tau\right), \quad C_2^3 = \frac{509}{6270}L_i\left(\frac{272}{10\,000}\tau\right),$$
$$C_1^3 = -\frac{11}{162}L_i\left(\frac{449}{10\,000}\tau\right) + \frac{1}{12}L_i\left(\frac{2}{100}\tau\right),$$
$$C_1^2 = \frac{89}{648}L_i\left(\frac{555}{10\,000}\tau\right). \tag{A8}$$

(ix) The transition $F_g = 2 \rightarrow F_e = 1,2,3$ of ^{85}Rb atoms for the σ^+–σ^- polarization configuration:

$$S_3 = \frac{7}{81}L_i\left(\frac{252}{10\,000}\tau\right), \quad S_2 = \frac{57\,043}{2\,708\,640}L_i\left(\frac{850}{10\,000}\tau\right),$$
$$S_1 = -\frac{5}{48}L_i\left(\frac{399}{10\,000}\tau\right), \quad C_2^3 = \frac{11\,299}{62\,700}L_i\left(\frac{684}{10\,000}\tau\right),$$
$$C_1^3 = \frac{47}{324}L_i\left(\frac{681}{10\,000}\tau\right), \quad C_1^2 = -\frac{1\,177\,019}{13\,543\,200}L_i\left(\frac{123}{1000}\tau\right). \tag{A9}$$

(x) The transition $F_g = 2 \rightarrow F_e = 1,2,3$ of ^{85}Rb atoms for the $\pi||\pi$ polarization configuration:

$$S_3 = \frac{864}{10\,000}L_i\left(\frac{575}{10\,000}\tau\right), \quad S_2 = \frac{35}{324}L_i\left(\frac{655}{10\,000}\tau\right),$$
$$S_1 = \frac{1}{12}L_i\left(\frac{661}{10\,000}\tau\right), \quad C_2^3 = \frac{136}{1000}L_i\left(\frac{547}{10\,000}\tau\right),$$
$$C_1^3 = \frac{108}{1000}L_i\left(\frac{587}{10\,000}\tau\right), \quad C_1^2 = -\frac{1733}{15\,390}L_i\left(\frac{805}{10\,000}\tau\right). \tag{A10}$$

(xi) The transition $F_g = 2 \rightarrow F_e = 1,2,3$ of ^{85}Rb atoms for the $\pi \perp \pi$ polarization configuration:

$$S_3 = \frac{864}{10\,000}L_i\left(\frac{580}{10\,000}\tau\right), \quad S_2 = \frac{833}{36\,936}L_i\left(\frac{310}{10\,000}\tau\right),$$
$$S_1 = -\frac{1}{24}L_i\left(\frac{661}{10\,000}\tau\right), \quad C_2^3 = \frac{155}{1000}L_i\left(\frac{563}{10\,000}\tau\right),$$
$$C_1^3 = \frac{71}{1000}L_i\left(\frac{572}{10\,000}\tau\right), \quad C_1^2 = \frac{3551}{30\,780}L_i\left(\frac{629}{10\,000}\tau\right). \tag{A11}$$

(xii) The transition $F_g = 3 \rightarrow F_e = 2,3,4$ of ^{85}Rb atoms for the σ^+–σ^+ polarization configuration:

$$S_4 = \frac{7}{12}L_i\,(s_0) - \frac{1}{3}L_i\left(\frac{265}{10\,000}\tau\right),$$
$$S_3 = \frac{101}{1000}L_i\left(\frac{638}{10\,000}\tau\right), \quad S_2 = \frac{5}{162}L_i\left(\frac{360}{10\,000}\tau\right),$$
$$C_3^4 = \frac{166}{1000}L_i\left(\frac{337}{10\,000}\tau\right), \quad C_2^4 = \frac{7385}{68\,688}L_i\left(\frac{125}{10\,000}\tau\right),$$
$$C_2^3 = \frac{125}{1000}L_i\left(\frac{203}{10\,000}\tau\right). \tag{A12}$$

(xiii) The transition $F_g = 3 \rightarrow F_e = 2,3,4$ of ^{85}Rb atoms for the σ^+–σ^- polarization configuration:

$$S_4 = \frac{1}{96}L_i\,(s_0) + \frac{11}{48}L_i\left(\frac{257}{10\,000}\tau\right),$$
$$S_3 = \frac{746}{10\,000}L_i\left(\frac{615}{10\,000}\tau\right), \quad S_2 = \frac{20}{4293}L_i\left(\frac{654}{100\,000}\tau\right),$$
$$C_3^4 = \frac{35}{864}L_i\,(s_0) + \frac{265}{1000}L_i\left(\frac{604}{10\,000}\tau\right), \tag{A13}$$
$$C_2^4 = \frac{5}{108}L_i\,(s_0) + \frac{1495}{8586}L_i\left(\frac{287}{10\,000}\tau\right),$$
$$C_2^3 = \frac{723}{10\,000}L_i\left(\frac{116}{10\,000}\tau\right).$$

(xiv) The transition $F_g = 3 \rightarrow F_e = 2,3,4$ of ^{85}Rb atoms for the $\pi||\pi$ polarization configuration:

$$S_4 = \frac{692}{1000}L_i\left(\frac{1716}{3217}s_0\right) - \frac{612}{10\,000}L_i\left(\frac{742}{10\,000}\tau\right),$$
$$S_3 = \frac{108}{1000}L_i\left(\frac{633}{10\,000}\tau\right), \quad S_2 = \frac{309}{10\,000}L_i\left(\frac{315}{10\,000}\tau\right),$$
$$C_3^4 = \frac{287}{10\,000}L_i\left(\frac{1716}{3217}s_0\right) + \frac{241}{1000}L_i\left(\frac{392}{10\,000}\tau\right),$$
$$C_2^4 = \frac{112}{1000}L_i\left(\frac{1716}{3217}s_0\right) + \frac{182}{1000}L_i\left(\frac{288}{10\,000}\tau\right),$$
$$C_2^3 = \frac{416}{10\,000}L_i\left(\frac{230}{10\,000}\tau\right). \tag{A14}$$

(xv) The transition $F_g = 3 \rightarrow F_e = 2,3,4$ of ^{85}Rb atoms for the $\pi \perp \pi$ polarization configuration:

$$S_4 = \frac{178}{1000} L_i\left(\frac{1716}{3217} s_0\right) + \frac{306}{10\,000} L_i\left(\frac{742}{10\,000}\tau\right),$$

$$S_3 = \frac{650}{10\,000} L_i\left(\frac{270}{10\,000}\tau\right), \quad S_2 = \frac{151}{10\,000} L_i\left(\frac{289}{10\,000}\tau\right),$$

$$C_3^4 = \frac{148}{1000} L_i\left(\frac{1716}{3217} s_0\right) + \frac{155}{1000} L_i\left(\frac{371}{10\,000}\tau\right), \quad \text{(A15)}$$

$$C_2^4 = \frac{309}{10\,000} L_i\left(\frac{1716}{3217} s_0\right) + \frac{156}{1000} L_i\left(\frac{310}{10\,000}\tau\right),$$

$$C_2^3 = \frac{12}{100} L_i\left(\frac{339}{10\,000}\tau\right).$$

[1] W. Demtröder, *Laser Spectroscopy* (Springer, Berlin, 1998).
[2] S. J. Park, H. S. Lee, H. Cho, and J. D. Park, J. Korean Phys. Soc. **33**, 281 (1998).
[3] S. Banerjee and V. Natarajan, Opt. Lett. **28**, 1912 (2003).
[4] V. Wong, R. W. Boyd, C. R. Stroud Jr., R. S. Bennink, and A. M. Marino, Phys. Rev. A **68**, 012502 (2003).
[5] S. Chakrabarti, A. Pradhan, A. Bandyopadhyay, A. Ray, B. Ray, N. Kar, and P. N. Ghosh, Chem. Phys. Lett. **399**, 120 (2004).
[6] S. Chakrabarti, A. Pradhan, B. Ray, and P. N. Ghosh, J. Phys. B **38**, 4321 (2005).
[7] F. Magnus, A. L. Boatwright, A. Flodin, and R. C. Shiell, J. Opt. B **7**, 109 (2005).
[8] A. Narayanan, Eur. Phys. J. D **39**, 13 (2006).
[9] D. Bhattacharyya, B. Ray, and P. N. Ghosh, J. Phys. B **40**, 4061 (2007).
[10] D. Bhattacharyya, A. Bandyopadhyay, S. Chakrabarti, B. Ray, and P. N. Ghosh, Chem. Phys. Lett. **440**, 24 (2007).
[11] A. Hernández-Hernández, E. Méndez-Martínez, A. Reyes-Reyes, J. Flores-Mijangos, J. Jiménez-Mier, M. López, and E. de Carlos, Opt. Commun. **282**, 887 (2009).
[12] P. G. Pappas, M. M. Burns, D. D. Hinshelwood, M. S. Feld, and D. E. Murnick, Phys. Rev. A **21**, 1955 (1980).
[13] H. Rinneberg, T. Huhle, E. Matthias, and A. Timmermann, Z. Phys. A **295**, 17 (1980).
[14] R. Grimm and J. Mlynek, Appl. Phys. B **49**, 179 (1989).
[15] O. Schmidt, K. M. Knaak, R. Wynands, and D. Meschede, Appl. Phys. B **59**, 167 (1994).
[16] K. B. Im, H. Y. Jung, C. H. Oh, S. H. Song, P. S. Kim, and H. S. Lee, Phys. Rev. A **63**, 034501 (2001).
[17] D. A. Smith and I. G. Hughes, Am. J. Phys. **72**, 631 (2004).
[18] L. P. Maguire, R. M. W. van Bijnen, E. Mese, and R. E. Scholten, J. Phys. B **39**, 2709 (2006).
[19] S. Lee, K. Lee, and J. Ahn, Jpn. J. Appl. Phys. **48**, 032301 (2009).
[20] M. Himsworth and T. Freegarde, Phys. Rev. A **81**, 023423 (2010).
[21] K. B. MacAdam, A. Steinbach, and C. E. Wieman, Am. J. Phys. **60**, 1098 (1992).
[22] A. K. Singh, L. Muanzuala, and V. Natarajan, e-print arXiv:1008.3228 [atom-ph].
[23] S. Nakayama, Jpn. J. Appl. Phys. **24**, 1 (1985).
[24] G. Moon and H. R. Noh, J. Korean Phys. Soc. **50**, 1037 (2007).
[25] G. Moon and H. R. Noh, Phys. Rev. A **78**, 032506 (2008).
[26] G. Moon and H. R. Noh, J. Opt. Soc. Am. B **25**, 701 (2008).
[27] G. Moon and H. R. Noh, J. Opt. Soc. Am. B **27**, 1741 (2010).
[28] A. R. Edmonds, *Angular Momentum in Quantum Mechanics* (Princeton University Press, Princeton, NJ, 1960).
[29] J. Sagle, R. K. Namiotka, and J. Huennekens, J. Phys. B **29**, 2629 (1996).
[30] G. Moon and H. R. Noh, J. Korean Phys. Soc. **54**, 13 (2009).
[31] G. Moon and H. R. Noh, Opt. Commun. **281**, 294 (2008).